Supporting Information

Selenium-substituted core and synergistic regioisomer-free monomethylated terminal enable methylated acceptor with efficiency and low energy loss in binary organic solar cells

Can Yang,[a,c,†] Tao Liu,[b,*,†] Kai-Kai Liu,[a] Lu Yan,[a] Asif Mahmood,[a] Min Gyu Kang,[d] Hongchen Rong,[a] Han Young Woo,[d] and Jin-Liang Wang [a,*]

[a] Key Laboratory of Cluster Science of the Ministry of Education, Beijing Key Laboratory of Intelligent Molecular Materials and High-throughput Manufacturing, School of Chemistry and Chemical Engineering, Beijing Institute of Technology, Beijing 100081, China

E-mail: jinlwang@bit.edu.cn

[b] School of Resources, Environment and Materials, Guangxi University, Nanning 530004, China

[c] College of Chemistry, Zhengzhou University, Zhengzhou 450001, China

[d] Department of Chemistry, Korea University, Seoul 136-713, Republic of Korea

†Can Yang and Tao Liu have contributed equally to this work.

1. Supplementary Experimental Section

1.1. Materials and Characterization

All air and water-sensitive reactions were carried out under N_2. THF, toluene, and diethyl ether were dried by Na and then freshly distilled before use. The other precursors were used as the common commercial level. ^1H and ^{13}C NMR spectra were carried out on a Bruker Ascend-400 and 700 NMR spectrometer. All chemical shifts were reported in ppm. Chemical shifts in ^1H NMR were referenced to TMS, and in ^{13}C NMR were referenced to $CDCl_3$. The peak positions of ^{13}C NMR were marked by groups. MALDI-TOF-MS was recorded on a Bruker BIFLEX III mass spectrometer. Thermogravimetric analysis (TGA) was performed using a TA Instrument Q600 analyzer under nitrogen gas flow with a heating rate of 10 ºC min^{-1}. UV-vis absorption spectra were taken on a Hitachi UH5300 UV-vis spectrometer. The electrochemical cyclic voltammetry was carried out on a CHI electrochemical workstation with a glass carbon disk, Ag/Ag^+ electrode, and Pt wire, as working electrode, reference electrode, and counter electrode, respectively, in a 0.1 M tetrabutylammonium hexafluorophosphate (Bu_4NPF_6) acetonitrile solution. During CV measurements, the films were drop-cast on the glass carbon working electrode from a $CHCl_3$ solution. Single-crystal data collection of **IT-M-γ** and **BIT-M-γ** was performed at 293 K on a Super Nova diffractometer, using graphite-monochromated Cu Kα radiation (λ=1.54184 Å). All calculations were performed using the SHELXL and the crystallographic software package. There is no A-alert in the CIF file of single crystal data. Crystallographic data have been deposited with the Cambridge Crystallographic Data Centre as supplementary publication No. CCDC 2173351 and 2173360 for **IT-M-γ** and **BIT-M-γ**, respectively. The single-crystal X-ray crystallographic data were summarized in **Table S1**.

1.2. BHJ-OSC Device Fabrication and Measurement

Devices were fabricated on the indium tin oxide (ITO) patterned glass with a conventional configuration of ITO/PEDOT: PSS/active layers/PDIN/Ag. The patterned indium tin oxide (ITO) glass-coated substrates (Size of 15*15*1mm, sheet resistance 15 Ω sq^{-1}) were consecutively cleaned in ultrasonic baths containing detergent, de-ionized water, and ethanol, respectively. Then, poly-(3,4-ethylenedioxythiophene):poly-(styrenesulphonic acid) (PEDOT:PSS) thin films (Heraeus Clevios P VP AI 4083) were fabricated on the cleaned ITO substrates by the spin-coating method at 5000 round per minute for 40 s, and then annealed at 150 °C for 10 minutes in ambient conditions. After annealing treatment, the ITO substrates coated PEDOT:PSS films were transferred to a high-purity nitrogen-filled glove box to fabricate active layers. **PM6**:**IT-M-γ** and **PM6**:**BIT-M-γ** blends (D: A=1:1.1, w/w) were dissolved in chloroform (CF) (the concentration of the blend solution was 16.8 mg mL^{-1}). The

blend solutions were spin-coated on PEDOT:PSS films in a high-purity nitrogen-filled glove box to fabricate the active layers. The optimal method for the active layer was to deposit the solution with 0.25% DIO (v/v) at ~3000 RPM and annealed at 80 °C for 5 minutes. The optimized thickness of the active layer is ~110 nm, which was measured by Ambios Technology XP-2 stylus Profiler. Atop the active layer, a thin electron transporting layer of PDIN (2 mg mL^{-1} in methanol with 0.25 vol% acetic acid, 5000 RPM for 30 s) was spin-coated. The cathode of Ag was deposited by thermal evaporation with a shadow mask under 10^{-4} Pa, and the thickness of 100 nm was monitored by a quartz crystal microbalance. The active area of OSCs is about 4 mm^2, which is defined by the overlap of ITO anode and Ag cathode. The current density-voltage (*J-V*) curves of polymer solar cells were measured in a high-purity nitrogen-filled glove box using a Keithley B2901A source meter. AM 1.5G irradiation at 100 mW cm^{-2} provided by a simulator (SS-F5-3A, Enlitech, AAA grade, 70×70 mm^2 photobeam size) in glove box, which was calibrated by standard silicon solar cells (purchased from Enlitech). The external quantum efficiency (EQE) spectra of polymer solar cells were measured in air conditions by a solar cell spectral response measurement system (QE-R3011, Enlitech).

1.3. Charge mobility measurement by SCLC method

The structure of electron-only devices is ITO/ZnO/active layer/PDIN/Al and the structure of hole-only devices is ITO/PEDOT:PSS/active layer/MoO_3/Ag. The fabrication conditions of the active layer films are same with those for the OSCs. The charge mobilities are generally described by the Mott-Gurney equation:[S1]

$$J = \frac{9}{8}\varepsilon_r\varepsilon_0\mu\frac{V^2}{L^3} \quad (1)$$

where J is the current density, ε_0 is the permittivity of free space (8.85×10^{-14} F/cm), ε_r is the dielectric constant of used materials, μ is the charge mobility, V is the applied voltage and L is the active layer thickness. The ε_r parameter is assumed to be 3, which is a typical value for organic materials. In organic materials, charge mobility is usually field dependent and can be described by the disorder formalism, typically varying with electric field, E=V/L, according to the equation:[S2]

$$\mu = \mu_0 \exp[0.89\gamma\sqrt{\frac{V}{L}}] \quad (2)$$

where μ_0 is the charge mobility at zero electric field and γ is a constant. Then, the Mott-Gurney equation can be described by:

$$J = \frac{9}{8}\varepsilon_r\varepsilon_0\mu_0\frac{V^2}{L^3}\exp[0.89\gamma\sqrt{\frac{V}{L}}] \quad (3)$$

In this case, the charge mobilities were estimated using the following equation:

$$\ln(\frac{JL^3}{V^2}) = 0.89\gamma\sqrt{\frac{V}{L}} + \ln(\frac{9}{8}\varepsilon_r\varepsilon_0\mu_0) \quad (4)$$

1.4. Morphology Characterization

The surface morphology of the active layers was investigated by atomic force microscopy (AFM) using a Dimension Icon AFM (Bruker) in tapping mode. The samples for AFM characterization were prepared under the same conditions as the active layers of OSCs. 2D Grazing-Incidence Wide-Angle X-ray Scattering (GIWAXS) measurements were carried out at the PLSII 9A U-SAXS beam line of Pohang Accelerator Laboratory, Korea. GIWAXS samples were prepared on PEDOT:PSS covered Si wafers in a similar manner to the devices of OSCs.

2. Supplementary Materials and Synthetic procedures of new compounds

***Materials*:** The precursor **IDTT-2CHO** and **IDTSe-2CHO** were synthesized according to the previous reports.[S3] PM6 was purchased from Solarmer Energy Inc. The detailed synthesis procedures of new compounds are as follows.

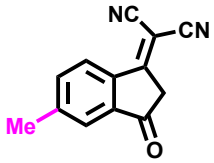

IC-M-γ

IC-M-γ: In a 250 mL two-neck round-bottom flask, compound **1** (6.000 g, 44.069 mmol) was added. The flask was evacuated and back-filled with N_2 three times, and then freshly distilled CH_2Cl_2 (80 mL), thionyl chloride (10.495 g, 88.138 mmol), and DMF (0.5 mL) were injected into the mixture. The resulting reaction mixture was stirred at 80 ℃ for 3 h under N_2 atmosphere. After removal of the solvent and excess thionyl chloride, the crude p-methylbenzoyl chloride (compound **2**) was obtained and used for the next reaction step directly. The flask was evacuated and back-filled with N_2 three times. Freshly distilled CH_2Cl_2 (50 mL) was injected, and anhydrous $AlCl_3$ (17.363 g, 132.207 mmol) was slowly added in batches and stirred at 0 ℃ for 15 minutes. After that, the mixture of freshly distilled CH_2Cl_2 (50 mL) and malonyl chloride (12.952 g, 88.138 mol) was added dropwise under N_2 atmosphere at 0 °C. After addition, the resulting reaction mixture was stirred at 80 °C for 12 h. After being cooled to room temperature, the mixture was quenched with oxalic acid solution and then extracted with ethyl acetate. The organic layers were combined and washed with saturated brine solution and dried over anhydrous Na_2SO_4. After removal of the solvent, the mixture was precipitated

with $NaHCO_3$ aqueous solution, washed with CH_2Cl_2, collected by filtration, and the crude product was obtained. After that, the crude compound **3** (2.330 g, 14.558 mmol) was directly transferred to a 100 mL two-neck flask without any purification, and then malononitrile (1.920 g, 29.116 mmol) was added. The anhydrous ethanol (20 mL) was injected to dissolve them, and then anhydrous sodium acetate (1.552 g, 18.925 mmol) was slowly added in batches. After that, the system color changed from purple to red, and the resulting reaction mixture was stirred at room temperature for 2 h. Then, dilute hydrochloric acid was added to adjust the pH of the reaction solution to acidic, producing a large amount of red and blue precipitates. The mixture was precipitated with water, then collected by filtration. The crude product was purified by silica gel column chromatography, eluting with petroleum ether/dichloromethane (1:2) to obtain the product as a light-yellow solid (**IC-M-*mix***). Then, regioisomer-free monomethylated terminal **IC-M-*γ*** as pink solid powder (0.909 g, 30%) was obtained by repeated recrystallization using anhydrous ethanol. ^{1}H NMR ($CDCl_3$, 400 MHz, ppm): δ 8.53-8.51 (d, J = 8.4 Hz, 1H, Ph-*H*), 7.77 (s, 1H, Ph-*H*), 7.70-7.68 (d, J = 8.4 Hz, 1H, Ph-*H*), 3.70 (s, 2H, CH_2), 2.57 (s, 3H, CH_3).

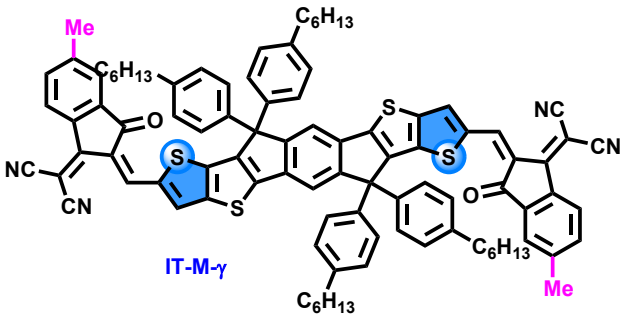

IT-M-γ

IT-M-*γ*: In a 100 mL two-neck round-bottom flask, **IDTT-2CHO** (50 mg, 0.047 mmol), **IC-M-*γ*** (48 mg, 0.23 mmol) was added. The reaction mixture was evacuated and backfilled with N_2 three times, and then freshly degassed chloroform (10 mL) and pyridine (0.5 mL) were added to the reaction mixture. The reaction mixture was stirred at room temperature for 12 h. Then the mixture was poured into methanol, and the precipitate was filtered off and washed with methanol. The crude product was purified by silica gel column chromatography, eluting with petroleum ether/dichloromethane (1:2) to give the product as a blue-black solid (60 mg, 90%). ^{1}H NMR ($CDCl_3$, 400 MHz, ppm): δ 8.82 (s, 2H, C=C*H*), 8.56-8.54 (d, J = 8.0 Hz, 2H, Ph-*H*), 8.21 (s, 2H, Ph-*H*), 7.70 (s, 2H, Th-*H*), 7.63 (s, 2H, Ph-*H*), 7.56-7.54 (d, J = 8.0 Hz, 2H, Ph-*H*), 7.23-7.21 (d, J = 8.0 Hz, 8H, Ph-*H*), 7.15-7.13 (d, J = 8.0 Hz, 8H, Ph-*H*), 2.59-2.55 (t, 8H, J = 7.2 Hz, CH_2), 2.53 (s, 6H, CH_3), 1.62-1.55 (m, 8H, CH_2), 1.36-1.28 (m, 24H, CH_2), 0.87-0.84 (t, J = 6.0 Hz, 12H, CH_3). ^{13}C NMR ($CDCl_3$, 175 MHz, ppm): δ 188.2, 160.3, 155.5,

152.5, 147.6, 146.7, 146.2, 143.5, 142.4, 139.5, 139.0, 137.8, 137.6, 137.2, 136.9, 136.5, 136.1, 128.8, 127.9, 125.2, 124.0, 123.2, 118.4, 114.7, 114.6, 68.5, 63.2, 35.6, 31.7, 31.2, 29.7, 29.2, 22.6, 22.0, 14.1.

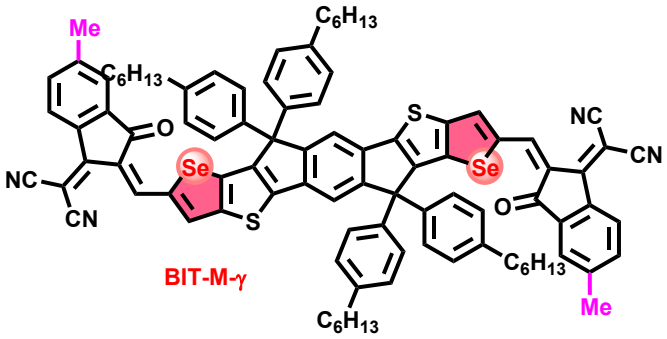

BIT-M-*γ*: In a 100 mL two-neck round-bottom flask, **IDTSe-2CHO** (50 mg, 0.043 mmol), **IC-M-*γ*** (44 mg, 0.214 mmol) was added. The reaction mixture was evacuated and backfilled with N_2 three times, and then freshly degassed chloroform (10 mL) and pyridine (0.5 mL) were added to the reaction mixture. The reaction mixture was stirred at room temperature for 12 h. Then the mixture was poured into methanol, and the precipitate was filtered off and washed with methanol. The crude product was purified by silica gel column chromatography, eluting with petroleum ether/dichloromethane (1:2) to give the product as a blue-black solid (60 mg, 90%). ^{1}H NMR ($CDCl_3$, 400 MHz, ppm): δ 8.98 (s, 2H, C=C*H*), 8.55-8.53 (d, J = 8.4 Hz, 2H, Ph-*H*), 8.23 (s, 2H, Ph-*H*), 7.67 (s, 4H, Se-*H,* Ph-*H*), 7.55-7.53 (d, J = 8.4 Hz, 2H, Ph-*H*), 7.22-7.20 (d, J = 8.0 Hz, 2H, Ph-*H*), 7.15-7.13 (d, J = 8.4 Hz, 8H, Ph-*H*), 2.59-2.55 (t, 8H, J = 7.6 Hz, CH_2), 2.52 (s, 6H, CH_3), 1.61-1.55 (m, 8H, CH_2), 1.35-1.26 (m, 24H, CH_2), 0.88-0.84 (t, J = 6.4 Hz, 12H, CH_3). ^{13}C NMR ($CDCl_3$, 175 MHz, ppm): δ 189.1, 160.0, 156.0, 152.4, 151.6, 149.9, 146.1, 144.7, 142.4, 141.1, 140.9, 140.2, 139.1, 137.6, 137.0, 136.1, 128.8, 127.9, 125.2, 124.0, 122.0, 118.6, 114.72, 114.65, 68.4, 63.1, 35.6, 31.7, 31.2, 29.7, 29.1, 22.5, 22.0, 14.1. MALDI-TOF MS (m/z): calcd. for $C_{96}H_{86}N_4O_2S_2Se_2$: 1550.5. Found: 1551.1.

3. Supplementary Figures, Tables, and Charts

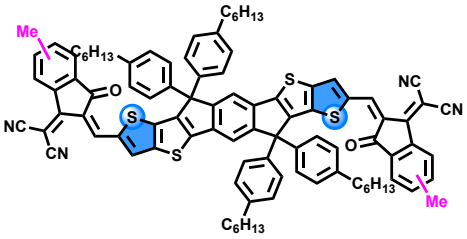

IT-M

Figure S1. The molecular structure of IT-M.

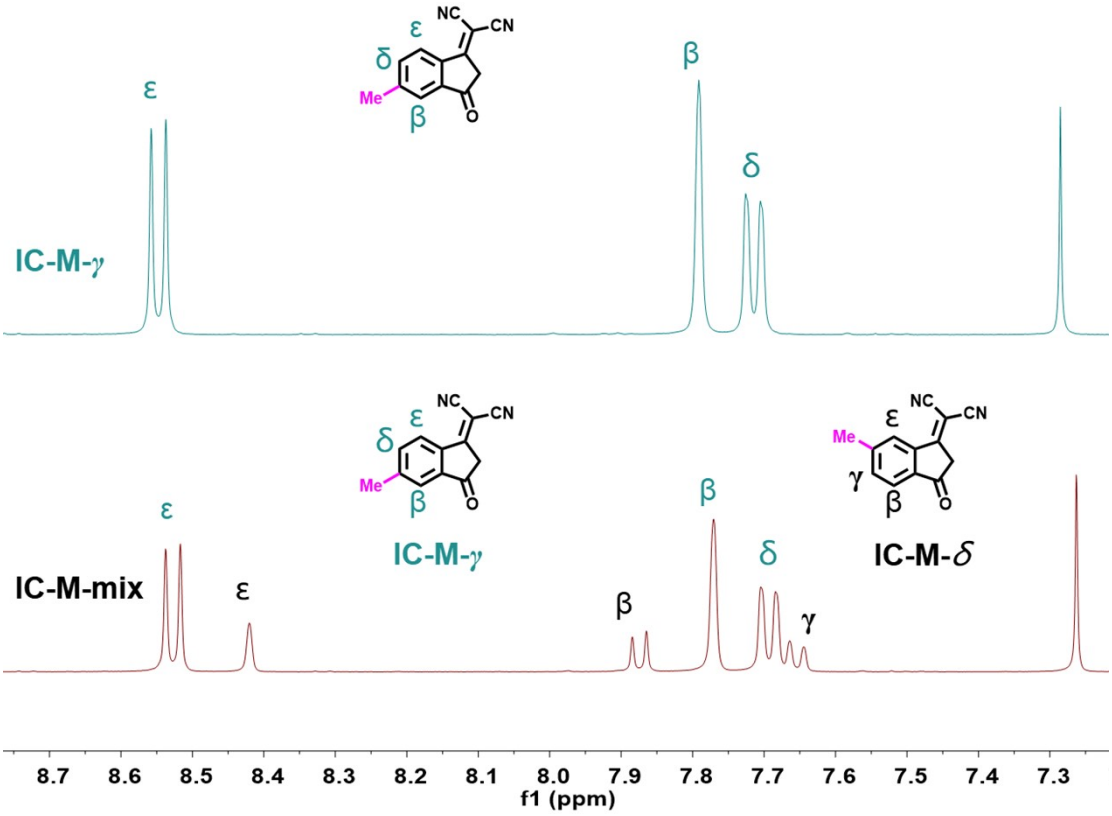

Figure S2. Partial ^{1}H NMR spectra (400 MHz, $CDCl_3$) of **IC-M-*γ*** and **IC-M-mix**.

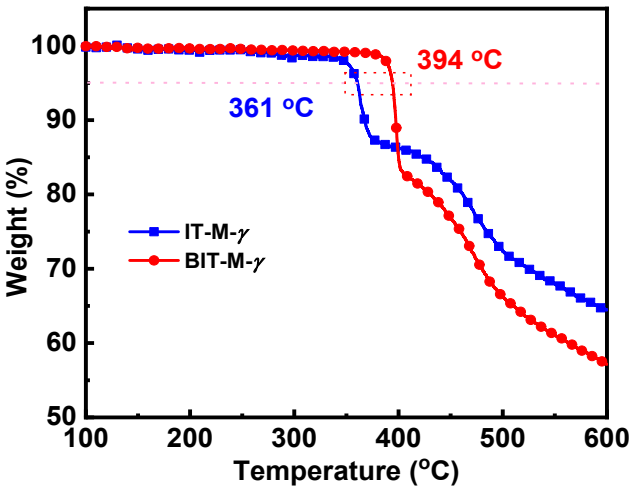

Figure S3. Thermal gravimetric analysis (TGA) of **IT-M-*γ*** and **BIT-M-*γ*** with a heating rate of 10 °C min^{-1} under N_2 atmosphere.

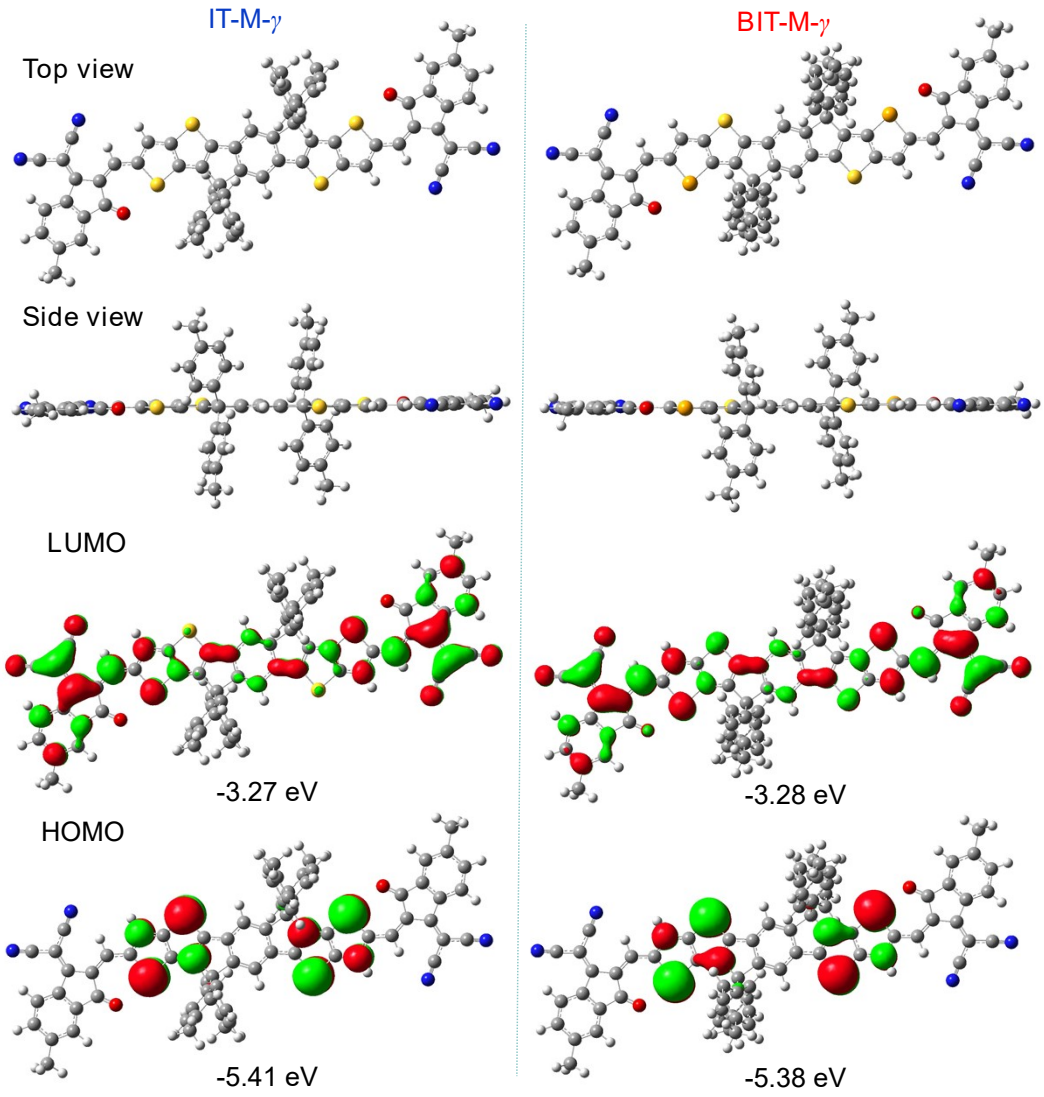

Figure S4. (a) The top and side views of molecular geometries, (b) The calculated LUMO and HOMO orbital distributions and energy levels for **IT-M-*γ*** and **BIT-M-*γ***, respectively.

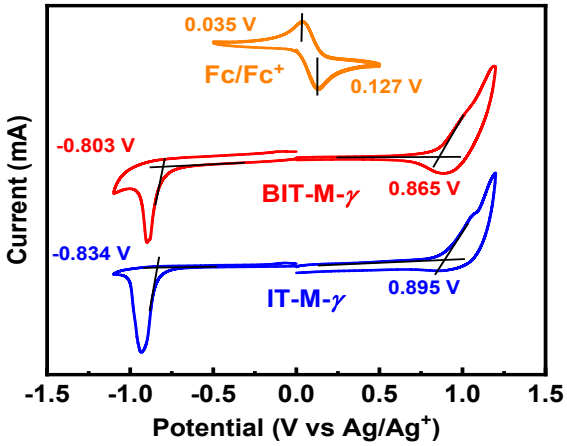

Figure S5. Cyclic voltammograms for **IT-M-*γ*** and **BIT-M-*γ*** films on a Pt electrode in 0.1 M Bu_4NPF_6 in CH_3CN solution, with the potential referenced to the Ag/Ag^+ reference electrode.

Table S1. Check CIF reports of single crystals of **IT-M-*γ*** and **BIT-M-*γ***.

Compound		**IT-M-*γ***	**BIT-M-*γ***
CCDC number		2173351	2173360
Temperature/K		293(2)	293(2)
Bond precision/Å		C-C=0.0026	C-C=0.0027
Unit cell dimensions	a/Å	15.4840(4)	8.3496(2)
	b/Å	17.9657(6)	16.1311(5)
	c/Å	21.3443(7)	35.9158(5)
	α/°	103.159(3)	101.247(2)
	β/°	110.252(3)	90.156(2)
	γ/°	99.365(2)	99.404(2)
Volume/Å^3		5231.2(3)	4677.8(2)
Crystal system		triclinic	triclinic
Space group		P -1	P -1
Empirical formula		$C_{96}H_{86}N_4O_2S_4$	$C_{96}H_{86}N_4O_2S_2Se_2$
Molecular weight		1455.93	1896.41
ρ_{calc}/g cm^{-3}		0.924	1.346
Z		2	2
μ/mm^{-1}		1.142	3.776
F(000)		1540.0	1922.0
h, k, l_{max}		19,22,26	10,20,44

Data completeness	0.919	0.933
Theta(max)	76.992	75.569
R(reflections)	0.1688(15891)	0.1143(16090)
wR_2(reflections)	0.4095(20329)	0.3059(18153)
S	0.943	1.060
Npar	961	1024

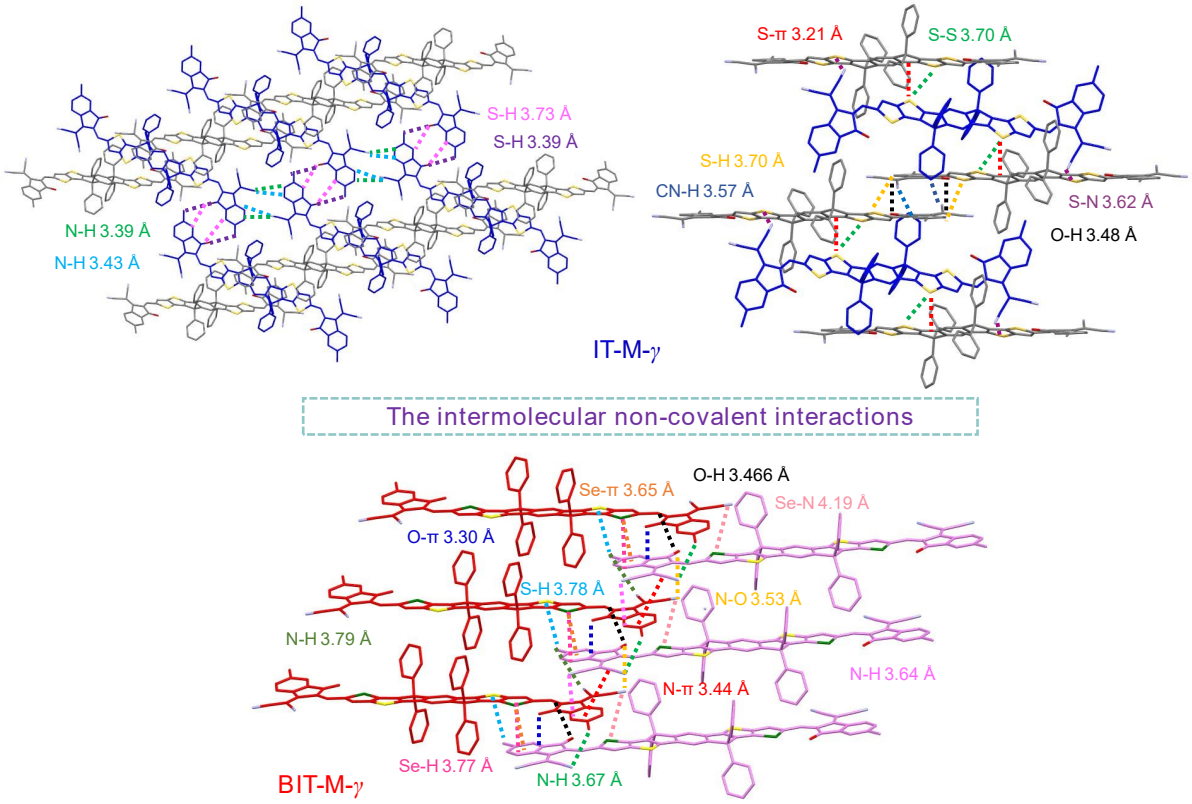

Figure S6. The intermolecular non-covalent interactions of **IT-M-*γ*** and **BIT-M-*γ*** crystals in one elliptical frame.

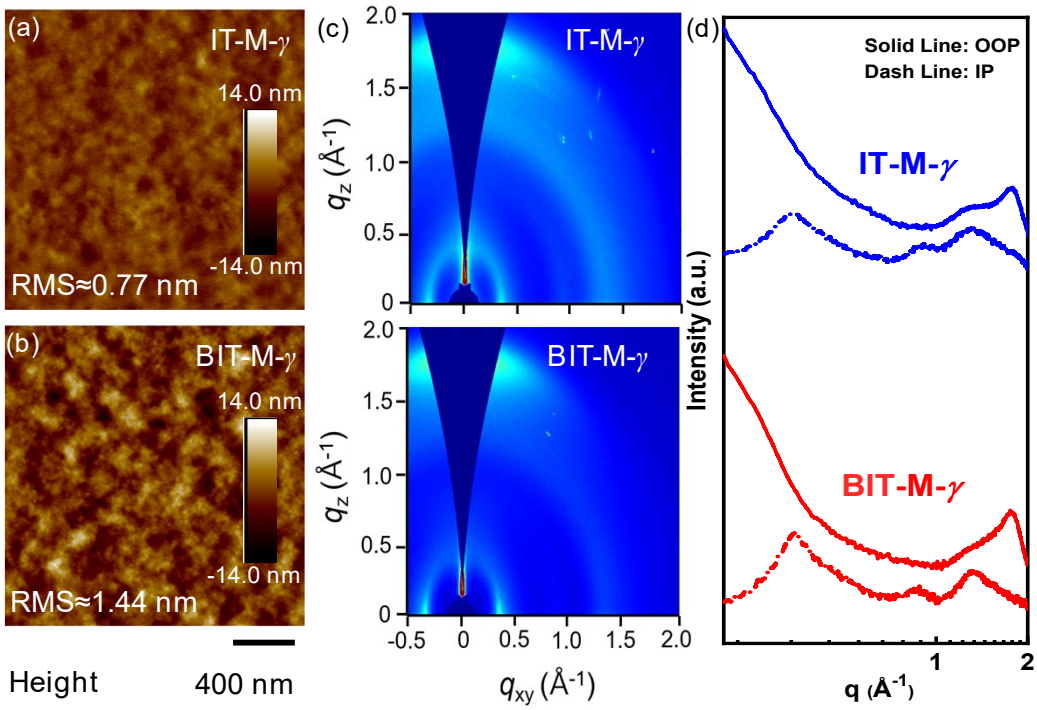

Figure S7. (a-b) AFM height images, (c) 2D-GIWAXS images of **IT-M-*γ*** and **BIT-M-*γ*** neat films; (d) The corresponding out-of-plane (solid curve) and in-plane (dashed curve) line-cut profiles of **IT-M-*γ*** and **BIT-M-*γ*** neat films.

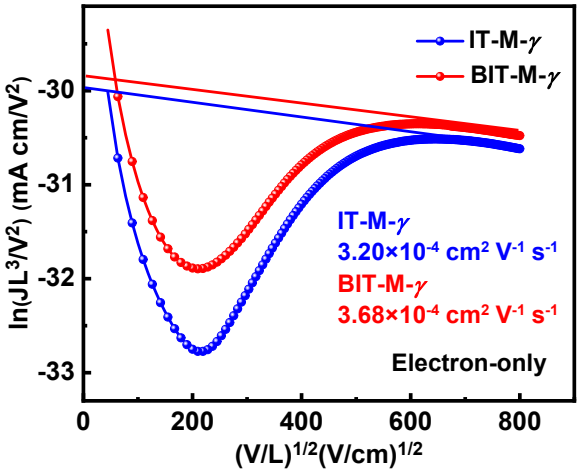

Figure S8. The $\ln(JL^3/V^2)$ vs $(V/L)^{0.5}$ curves for an electron-only device (ITO/ZnO/**IT-M-*γ*** or **BIT-M-*γ***/PDIN/Al) by the space-charge-limited current method.

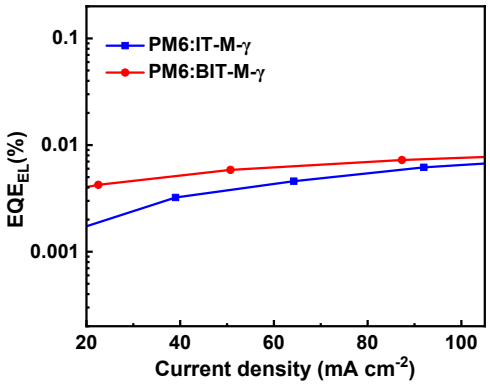

Figure S9. EQE_{EL} curves for devices based on **PM6:IT-M-γ** and **PM6:BIT-M-γ**.

Table S2. Summary of the photovoltaic parameters for recently reported A-D-A-type SMAs with methylated IC-based binary BHJ-OSCs.

Donor: Acceptor	V_{OC} (V)	J_{SC} (mA cm^{-2})	FF (%)	PCE (%)	E_g (eV)	E_{loss}（eV）	Ref.
PM6:IT-M-γ	**1.014**	**15.45**	**70.6**	**11.06**	**1.60**	**0.586**	**This work**
PM6:BIT-M-γ	**0.941**	**17.98**	**74.2**	**12.56**	**1.45**	**0.509**	**This work**
PBDB-T:IT-M	0.94	17.44	73.5	12.05	1.60	0.66	[S4]
PB3T:IT-M	1.00	18.9	63	11.9	1.60	0.6	[S5]
PBDB-T:IT-M	0.937	16.70	69.0	10.80	1.60	0.663	[S6]
J71:IT-M	0.981	17.71	61.5	10.68	1.60	0.619	[S7]
PTZ1:IT-M	0.98	14.9	62.2	9.1	1.60	0.62	[S8]
PTZ1:POIT-M	0.97	15.4	65.1	9.7	1.60	0.63	[S8]
PTZ1:MOIT-M	0.96	17.5	68.8	11.6	1.60	0.64	[S8]
PDTH-TZNT:IT-M	0.75	10.15	58.1	4.42	1.60	0.85	[S9]
PDTF-TZNT:IT-M	0.80	17.33	72.5	10.05	1.60	0.80	[S9]
FTAZ:IT-M	0.96	17.2	67.9	11.8	1.60	0.64	[S10]
PBDB-T:IT-M	0.94	13.5	52.8	7.2	1.60	0.66	[S10]
PBPTBz-2Cl:IT-M	0.99	14.92	48.61	7.18	1.60	0.61	[S11]
PBD:IT-M	1.00	13.97	59.6	8.33	1.60	0.60	[S12]
PBD2T:IT-M	0.89	15.95	72.8	10.34	1.60	0.71	[S12]
PBDB-T:IT-M	0.940	16.61	71.76	11.20	1.60	0.66	[S13]
PBDB-T:IT-M	0.94	16.18	71	10.90	1.60	0.66	[S14]
PBDB-T:IT-M	0.890	14.4	65	8.2	1.60	0.71	[S15]
PBDB-T:IT-M	0.952	16.59	67.5	11.15	1.60	0.648	[S16]

PBDB-T:IT-M	0.940	17.26	66.63	10.81	1.60	0.66	[S17]
PBDB-T:IT-M	0.94	17.17	71.46	11.71	1.60	0.66	[S18]
PTBTz-2:IT-M	0.954	17.61	61.84	10.51	1.60	0.646	[S19]
PFBT-T:IT-M	0.878	10.88	59.04	5.64	1.60	0.722	[S20]
PBZ-2Si:IT-M	0.88	17.69	71.55	11.14	1.60	0.72	[S21]
PBDB-T:IT-M	0.952	16.59	67.5	11.15	1.60	0.648	[S22]
PBDB-T:IT-M	0.92	16.09	68.44	10.11	1.60	0.68	[S23]
PBDB-TF:IT-M	1.02	14.35	51.55	7.51	1.60	0.58	[S24]
PBDB-T:ITIC-M	0.913	17.2	65.1	10.2	1.60	0.687	[S25]
PBDB-T:MeIC1	0.889	15.94	66.45	9.42	1.54	0.651	[S26]
J71:T6Me	0.82	21.85	62.88	11.26	1.38	0.56	[S27]
PBDB-T:IT-M	0.946	15.34	73.4	10.65	1.60	0.654	[S28]
PBDB-T:IT-M	0.92	16.30	71.6	10.73	1.60	0.68	[S29]
PFBT-T:IT-M	0.963	17.55	68.9	11.64	1.60	0.637	[S30]
PBDB-TF:IT-M	1.00	15.50	62.2	10.20	1.60	0.6	[S31]
PBDFP-Bz:IT-M	1.02	18.27	69.38	12.93	1.60	0.58	[S32]
PBDB-T:IDTT-OB	0.92	16.29	71.62	10.76	1.59	0.67	[S33]
PM6:ITIC-M	1.036	14.32	59.48	8.82	1.665	0.629	[S34]
PBDB-T:IT-M	0.930	14.590	65.703	8.883	1.60	0.67	[S35]
PBDB-T:SeInMe	0.91	15.90	61	8.80	/	/	[S36]
PBDB-T:SeOutMe	0.90	16.70	64	9.68	/	/	[S36]
PM6:MOIT-M	1.01	15.8	64.3	10.3	1.60	0.59	[S37]
PM6:IT-M	1.030	15.65	64.62	10.42	1.60	0.57	[S38]
PM6:IT-M	1.03	12.81	67.94	8.95	1.60	0.57	[S39]
PBDB-T:IT-SM	0.85	16.02	64	8.98	1.54	0.69	[S40]
PBDB-T:IT-DSM	0.88	12.54	49	5.65	1.59	0.71	[S40]
P3HT:CPDT-ICMe	0.77	16.52	65	8.17	/	/	[S41]
PM6:IT-M	1.022	15.21	60.11	9.35	1.60	0.578	[S42]

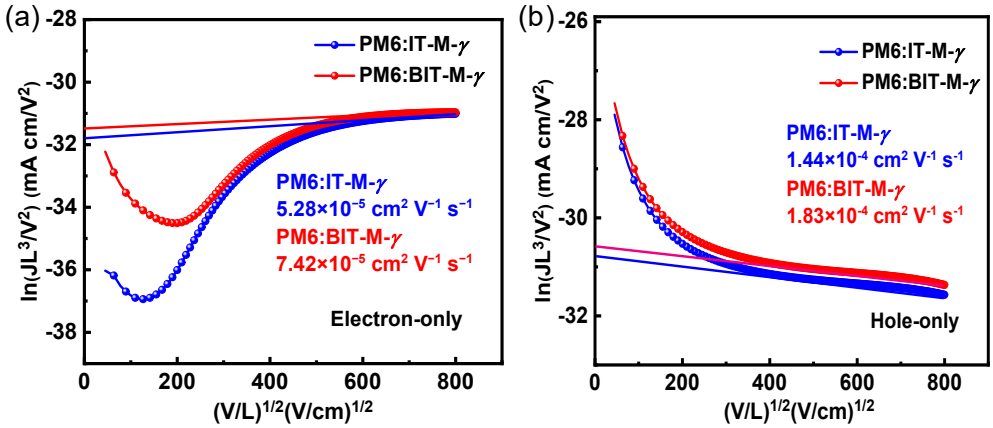

Figure S10. (a) The $\ln(JL^3/V^2)$ vs $(V/L)^{0.5}$ curves for an electron-only device (ITO/ZnO/**PM6**:**IT-M-γ** or **PM6**:**BIT-M-γ**/PDIN/Al) by the space-charge-limited current method. (b) The $\ln(JL^3/V^2)$ vs $(V/L)^{0.5}$ curves for hole-only devices (ITO/PEDOT:PSS/active layer/MoO_3/Ag) by the space-charge-limited current method.

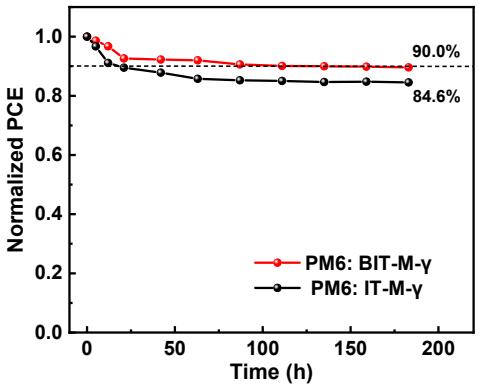

Figure S11. Normalized PCE of the **PM6:IT-M-γ** and **PM6:BIT-M-γ**-based OSCs as a function of annealing time at 80 °C in the nitrogen-filled glovebox.

4. $^{1}H/^{13}C$ NMR, and MALDI-TOF-MS Spectra of these acceptors

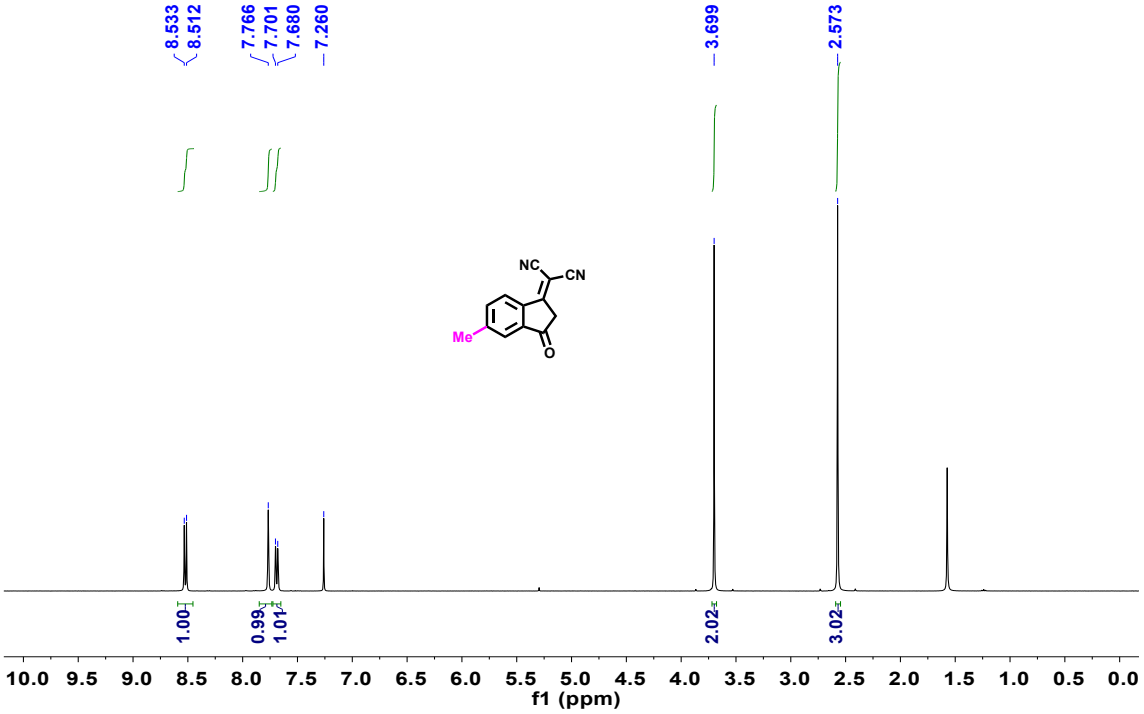

Figure S12. ^{1}H NMR spectrum for **IC-M-γ**

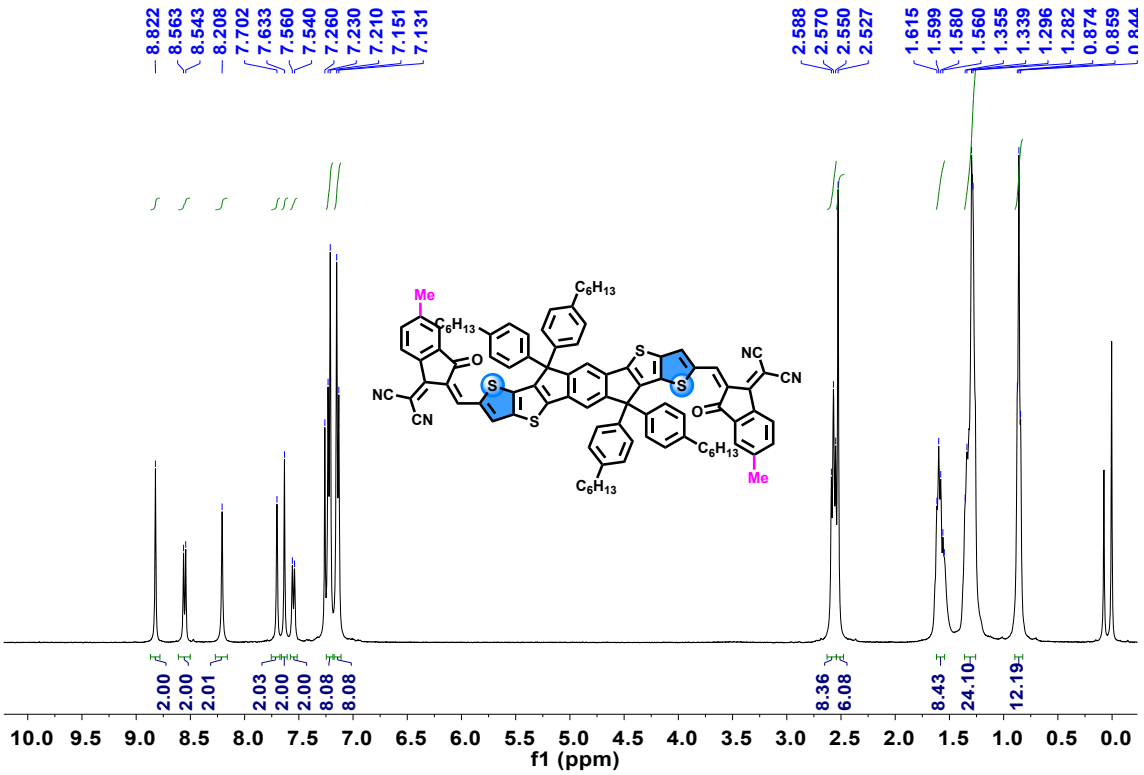

Figure S13. ^{1}H NMR spectrum for **IT-M-γ**

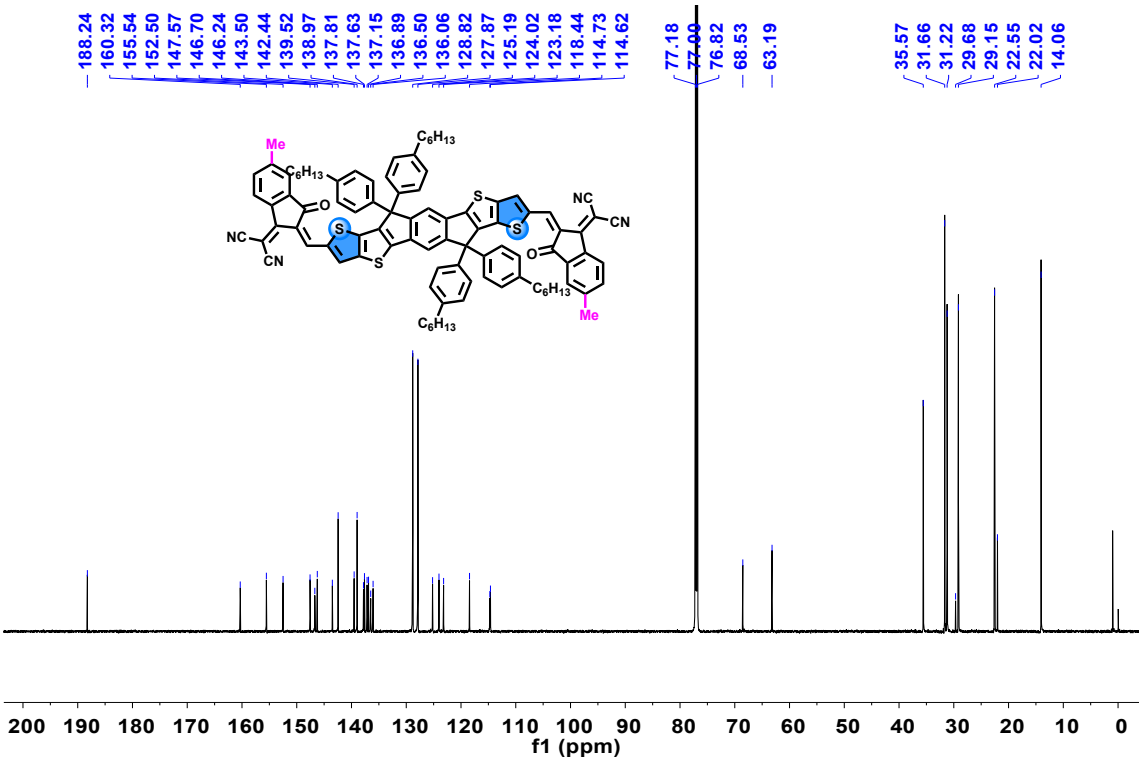

Figure S14. ^{13}C NMR spectrum for **IT-M-γ**

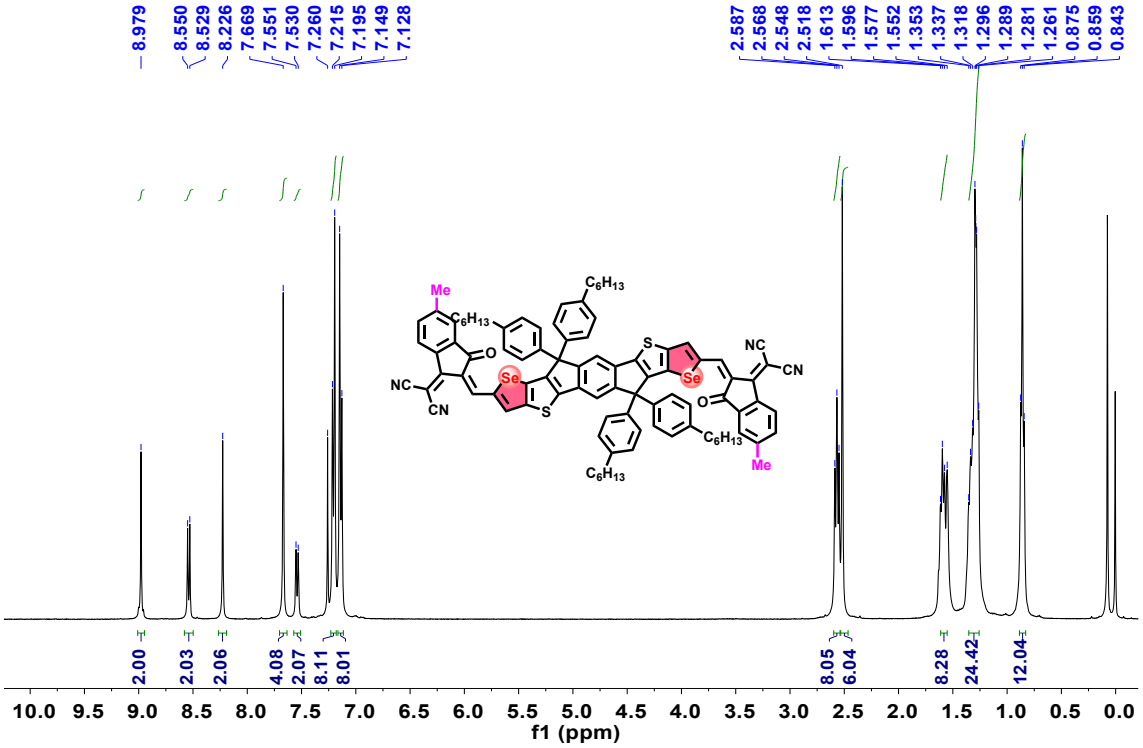

Figure S15. ^{1}H NMR spectrum for **BIT-M-γ**

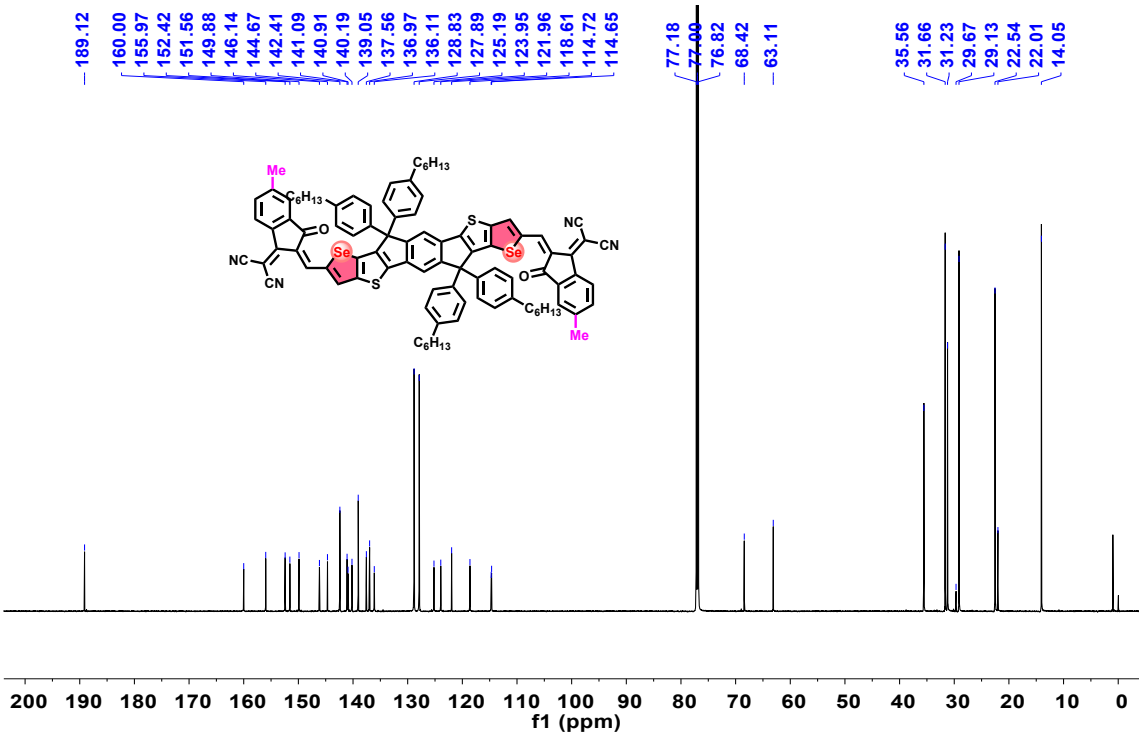

Figure S16. ^{13}C NMR spectrum for **BIT-M-γ**

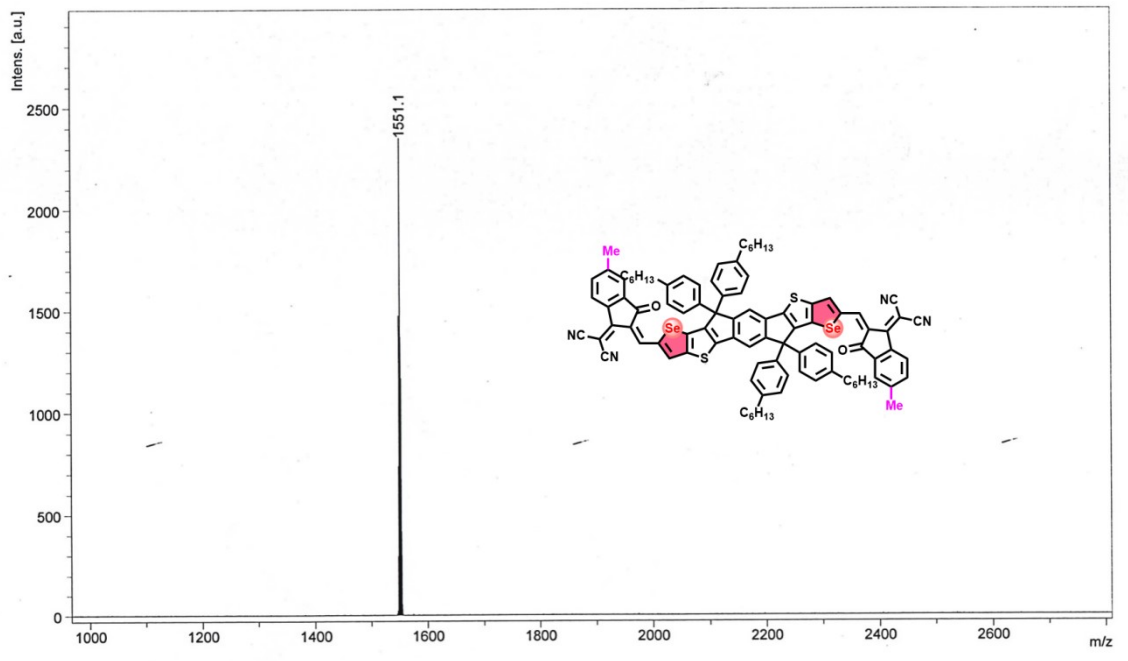

Figure S17. MALDI-TOF mass spectrum of **BIT-M-γ**

5. Supplementary References

[S1] Y. Zhang, D. Deng, K. Lu, J. Zhang, B. Xia, Y. Zhao, J. Fang, Z. Wei, *Adv. Mater.* **2015**, *27*, 1071-1076.

[S2] H. Cha, D. S. Chung, S. Y. Bae, M.-J. Lee, T. K. An, J. Hwang, K. H. Kim, Y.-H. Kim, D. H. Choi, C. E. Park, *Adv. Funct. Mater.* **2013**, *23*, 1556-1565.

[S3] K.-K. Liu, X. Xu, J. -L. Wang, C. Zhang, G. -Y. Ge, F.-D. Zhuang, H.-J. Zhang, C. Yang, Q. Peng, J. Pei, *J. Mater. Chem. A* **2019**, *7*, 24389-24399.

[S4] S. Li, L. Ye, W. Zhao, S. Zhang, S. Mukherjee, H. Ade, J. Hou, *Adv. Mater.* **2016**, *28*, 9423-9429.

[S5] D. Liu, B. Yang, B. Jang, B. Xu, S. Zhang, C. He, H. Y. Woo, J. Hou, *Energy Environ. Sci.* **2017**, *10*, 546-551.

[S6] W. Zhao, S. Li, S. Zhang, X. Liu, J. Hou, *Adv. Mater.* **2017**, *29*, 1604059.

[S7] Z. Hu, F. Zhang, Q. An, M. Zhang, X. Ma, J. Wang, J. Zhang, J. Wang, *ACS Energy Lett.* **2018**, *3*, 555-561.

[S8] W. Su, Q. Fan, X. Guo, J. Chen, Y. Wang, X. Wang, P. Dai, C. Ye, X. Bao, W. Ma, M. Zhang, Y. Li, *J. Mater. Chem. A* **2018**, *6*, 7988-7996.

[S9] D. Tang, J. Wan, X. Xu, Y. W. Lee, H. Y. Woo, K. Feng, Q. Peng, *Nano Energy* **2018**, *53*, 258-269.

[S10] H. Hu, L. Ye, M. Ghasemi, N. Balar, J. J. Rech, S. J. Stuard, W. You, B. T. O'Connor, H. Ade, *Adv. Mater.* **2019**, *31*, 1808279.

[S11] P. Chao, L. Liu, J. Qu, Q. He, S. Gan, H. Meng, W. Chen, F. He, *Dyes and Pigments* **2019**, *162*, 746-754.

[S12] Y. Gao, D. Li, Z. Xiao, X. Qian, J. Yang, F. Liu, S. Yang, L. Ding, *Mater. Chem. Front.* **2019**, *3*, 399-402.

[S13] B.-h. Yu, J. Wang, X.-l. Ma, S.-m. Zeng, S.-y. Hu, F.-j. Zhang, *Phys. Status Solidi RRL* **2019**, *13*, 1900217.

[S14] L. Wu, L. Xie, H. Tian, R. Peng, J. Huang, B. Fanady, W. Song, S. Tan, W. Bi, Z. Ge, *Sci. Bull.* **2019**, *64*, 1087-1094.

[S15] N. Y. Doumon, F. V. Houard, J. Dong, H. Yao, G. Portale, J. Hou, L. J. Koster, *Org. Electron.* **2019**, *69*, 255-262.

[S16] D. Yan, J. Xin, W. Li, S. Liu, H. Wu, W. Ma, J. Yao, C. Zhan, *ACS Appl. Mater. Interfaces* **2019**, *11*, 766-773.

[S17] Y. Bai, C. Zhao, Q. Guo, J. Zhang, S. Hu, J. Liu, T. Hayat, A. Alsaedi, Z.'a. Tan, *Org. Electron.* **2019**, *68*, 168-175.

[S18] L. Nian, Y. Kan, H. Wang, K. Gao, B. Xu, Q. Rong, R. Wang, J. Wang, F. Liu, J. Chen, G. Zhou, T. P. Russell, A. K. Y. Jen, *Energy Environ. Sci.* **2018**, *11*, 3392-3399.

[S19] Z. Liang, J. Tong, H. Li, Y. Wang, N. Wang, J. Li, C. Yang, Y. Xia, *J. Mater. Chem. A* **2019**, *7*, 15841-15850.

[S20] T. Lei, W. Song, B. Fanady, T. Yan, L. Wu, W. Zhang, L. Xie, L. Hong, Z. Ge, *Polymer* **2019**, *172*, 391-397.

[S21] H. Jiang, F. Pan, L. Zhang, X. Zhou, Z. Wang, Y. Nian, C. Liu, W. Tang, Q. Ma, Z. Ni, M. Chen, W. Ma, Y. Cao, J. Chen, *ACS Appl. Mater. Interfaces* **2019**, *11*, 29094-29104.

[S22] F. Shen, D. Yan, W. Li, H. Meng, J. Huang, X. Li, J. Xu, C. Zhan, *Mater. Chem. Front.* **2019**, *3*, 301-307.

[S23] M. Lv, Y. Li, X. Wei, Y. Xu, Z. Ge, X. Chen, *ACS Appl. Energy Mater.* **2019**, *2*, 2238-2245.

[S24] L. Zhan, S. Li, S. Zhang, T.-K. Lau, T. R. Andersen, X. Lu, M. Shi, C.-Z. Li, G. Li, H. Chen, *Sol. RRL* **2019**, *3*, 1900317.

[S25] H. Yin, K. L. Chiu, P. Bi, G. Li, C. Yan, H. Tang, C. Zhang, Y. Xiao, H. Zhang, W. Yu, H. Hu, X. Lu, X. Hao, S. K. So, *Adv. Energy Mater.* **2019**, *5*, 1900497.

[S26] X. Ma, M. Luo, W. Gao, J. Yuan, Q. An, M. Zhang, Z. Hu, J. Gao, J. Wang, Y. Zou, C. Yang, F. Zhang, *J. Mater. Chem. A* **2019**, *7*, 7843-7851.

[S27] J. Gao, R. Ming, Q. An, X. Ma, M. Zhang, J. Miao, J. Wang, C. Yang, F. Zhang, *Nano Energy* **2019,** *63*, 103888.

[S28] Y. Wang, C. Zhuang, Y. Fang, H. D. Kim, H. Yu, B. Wang, H. Ohkita, *Nanomaterials* **2020**, *10*, 241.

[S29] X. Guo, H. Li, Y. Han, Y. Yang, Q. Luo, C.-Q. Ma, J. Yang, *Org. Electron.* **2020**, *82*, 105725.

[S30] Y. Li, S. Zhou, Z. Xiong, M. Qin, K. Liu, G. Cai, H. Wang, S. Zhao, G. Li, Y.-J. Hsu, J. Xu, X. Lu, *ACS Appl. Energy Mater.* **2020**, *3*, 11359-11367.

[S31] Z. Li, X. Li, Q. Yang, K. Ren, G. Nian, Z. Xie, *Org. Electron.* **2020**, *81*, 105690.

[S32] Y. Gao, Z. Shen, F. Tan, G. Yue, R. Liu, Z. Wang, S. Qu, Z. Wang, W. Zhang, *Nano Energy* **2020**, *76*, 104964.

[S33] M. Li, Y. Zhou, M. Zhang, Y. Liu, Z. Ma, F. Liu, R. Qin, Z. Bo, *Sol. RRL* **2021**, *5*, 2100806.

[S34] Y. Zeng, D. Li, H. Wu, Z. Chen, S. Leng, T. Hao, S. Xiong, Q. Xue, Z. Ma, H. Zhu, Q. Bao, *Adv. Funct. Mater.* **2022**, *32*, 2110743.

[S35] Z. Chen, H. Chen, C. Feng, X. Wang, Z. He, Y. Cao, *J. Mater. Chem. C* **2021**, *9*, 7658-7664.

[S36] C. Labanti, M. J. Sung, J. Luke, S. Kwon, R. Kumar, J. Hong, J. Kim, A. A. Bakulin, S.-K. Kwon, Y.-H. Kim, J.-S. Kim, *ACS Nano* **2021**, *15*, 7700-7712.

[S37] X. Yan, J. Wu, J. Lv, L. Zhang, R. Zhang, X. Guo, M. Zhang, *J. Mater. Chem. A* **2022**, *10*, 15605-15613.

[S38] J. Gao, X. Ma, C. Xu, X. Wang, J. H. Son, S. Y. Jeong, Y. Zhang, C. Zhang, K. Wang, L. Niu, J. Zhang, H. Y. Woo, J. Zhang, F. Zhang, *Chem. Eng. J.* **2022**, *428*, 129276.

[S39] X. Wang, X. Zhai, X. Jing, C. Gao, Y. He, L. Yu, M. Sun, *Chem. Eng. J.* **2022**, *427*, 132048.

[S40] S. Jeong, H. Je, J. H. Lee, S. H. Lee, S.-Y. Jang, K. Park, H. Kang, S.-K. Kwon, Y.-H. Kim, K. Lee, *Dyes and Pigments* **2022**, *198*, 109987.

[S41] D. Han, Y. Han, Y. Kim, J.-W. Lee, D. Jeong, H. Park, G.-U. Kim, F. S. Kim, B. J. Kim, *J. Mater. Chem. A* **2022**, *10*, 640-650.

[S42] Z. Zhang, Y. Zhang, Z. Deng, T. Huang, D. Wang, X. Zhang, Q. Liao, J. Zhang, *J. Mater. Chem. A* **2023**, *11*, 23354-23359.